Appl Phys B (2011) 102: 31–35
DOI 10.1007/s00340-010-4092-9

Applied Physics B
Lasers and Optics

Optimally-output-coupled, 17.5 W, fiber-laser-pumped continuous-wave optical parametric oscillator

S. Chaitanya Kumar · R. Das · G.K. Samanta · M. Ebrahim-Zadeh

Received: 22 March 2010 / Revised version: 30 April 2010 / Published online: 12 June 2010

Abstract We present a stable, high-power, fiber-laser-pumped, continuous-wave (cw), singly resonant optical parametric oscillator (SRO) for the mid-infrared in an output-coupled (OC) configuration, providing 17.5 W of total output power at 61% extraction efficiency. Using a single-frequency, cw Yb fiber laser at 1064 nm and a 50-mm-long MgO:PPLN crystal, through optimization of signal output coupling we generate up to 9.8 W of signal power in the near-infrared together with 7.7 W of idler power for 28.6 W of pump, while in the absence of output coupling, 8.6 W of idler power is generated for the same pump power at 30% efficiency. The SRO is tunable over 360 nm in the idler range. The deployment of signal output coupling results in a total tuning of 513 nm (120 nm of signal, 393 nm of idler) over which watt-level output power can be extracted. Through careful control of thermal effects we achieve a long-term peak-to-peak idler power stability of 5% over 14 hours near room temperature. The output beams have TEM_{00} spatial profile with $M^2 < 1.28$ for the idler and $M^2 < 1.37$ for the signal.

1 Introduction

Continuous-wave (cw), singly resonant optical parametric oscillators (SROs) have been established as viable sources of high-power, widely tunable radiation in the near- to mid-infrared (IR) for a variety of applications such as spectroscopy and trace gas sensing [1]. When combined with the recent advances in fiber laser technology, they offer a viable route to the realization of compact, portable, robust, and cost-effective sources, potentially capable of providing multiwatt output powers at high efficiency. Earlier efforts on the development of cw SROs have exploited the most widely established quasi-phase-matched nonlinear material, periodically poled $LiNbO_3$ (PPLN) and MgO:PPLN [1–9]. In cw SROs, various wavelength tuning protocols have been implemented and are by now well-established. Coarse wavelength tuning can be obtained by changing the grating period [6] or varying the temperature of the nonlinear crystal [7], while continuous, mode-hop-free, fine tuning can be achieved by using an etalon in the cavity [6]. Rapid and continuous mode-hop-free tuning of up to 110 GHz around 3.4 μm has also been demonstrated by tuning a diode-amplified fiber pump laser [8]. Another tuning method based on the use of a diffraction grating has also been recently reported [9]. On the other hand, the attainment of high optical powers in the near- and mid-IR remains an experimentally challenging task, essentially due to heavy thermal loading of the nonlinear crystal resulting from the high intracavity signal power at increased pump powers. This can lead to effects such as thermally induced optical bistability [3], saturation, and subsequently a substantial drop in efficiency, thus limiting the available output power [4]. To date, a maximum of 10 W of idler at 3 μm from 50 W of pump at 20% efficiency has been achieved in a cw SRO [2]. In order to increase the extraction efficiency, various schemes such as signal output coupling [5, 11] and intracavity frequency doubling [12] have been employed to minimize thermal effects, hence retaining high output power. Implementation of output coupling has also extended the tuning range together

S. Chaitanya Kumar (✉) · R. Das · G.K. Samanta · M. Ebrahim-Zadeh
ICFO-Institut de Ciencies Fotoniques, Mediterranean Technology Park, 08860 Castelldefels, Barcelona, Spain
e-mail: chaitanya.suddapalli@icfo.es
Fax: +34-935-534000

M. Ebrahim-Zadeh
Institucio Catalana de Recerca i Estudis Avancats (ICREA), Passeig Lluis Companys 23, Barcelona 08010, Spain

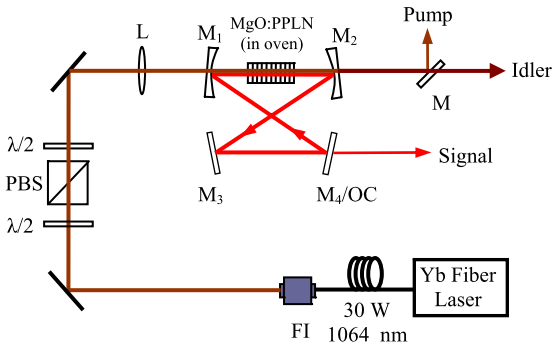

Fig. 1 Experimental setup for Yb fiber-laser-pumped, high-power cw OC-SRO based on MgO:PPLN crystal. FI: Faraday isolator, $\lambda/2$: half-wave plate, PBS: polarizing beamsplitter, L: lens, M: dichroic mirror

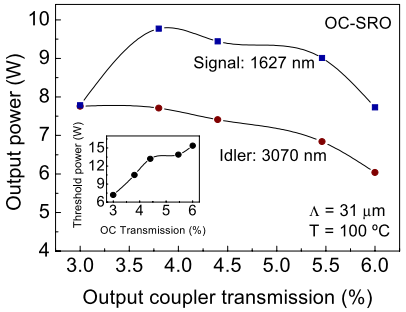

Fig. 2 Variation of extracted signal (1627 nm) and idler (3070 nm) power with OC transmission. *Inset*: Variation of threshold pump power with OC transmission

with improved extraction efficiency up to 59%, resulting in a total power of 8.6 W (5.1 W signal, 3.5 W idler) for 15 W of pump power [5]. Hence, optimization of output coupling becomes a critical issue for power scaling of cw SROs to multiwatt levels, while maintaining output stability and extraction efficiency.

Here we describe a stable and high-power cw SRO for the near- to mid-IR based on MgO:PPLN, which can provide as much as 17.5 W of total power (9.8 W signal, 7.7 W idler) at an overall extraction efficiency of 61%, by deploying optimized signal output coupling. The cw SRO delivers an idler power with a peak-to-peak power stability of 5% over 14 hours in a TEM_{oo} spatial profile. We also compare the performance of the device with the conventional cw SRO in the absence of signal output coupling. To the best of our knowledge, this is the highest total power and good long-term power stability, achieved to date from a cw OPO based on MgO:PPLN.

2 Experimental set-up

A schematic of the experimental setup is shown in Fig. 1. The pump source is a cw, single-frequency Yb fiber laser (IPG Photonics, YLR-30-1064-LP-SF), delivering up to 30 W at 1064 nm in a linearly polarized beam of 4 mm diameter in TEM_{00} spatial mode ($M^2 < 1.01$), with a nominal linewidth of 89 kHz. In order to maintain stable output characteristics, the laser is operated at maximum power and a combination of a half-wave plate and polarizing beamsplitter is used as variable attenuator. A second half-wave plate controls the polarization for phase-matching in the nonlinear crystal. The nonlinear crystal is a 50-mm-long, 1-mm-thick, 5% MgO:PPLN with five grating periods ($\Lambda = 29.5$ to 31.5 μm, in steps of 0.5 μm). The crystal is housed in an oven with a stability of ±0.1°C, which can be tuned from room temperature to 200°C. The SRO cavity is a symmetric ring, comprising two concave mirrors, M_1 and M_2 ($r = 150$ mm), and two plane mirrors, M_3 and M_4. All mirrors have high reflectivity ($R > 99\%$) over 1.3–1.9 μm and high transmission ($T > 90\%$) over 2.2–4 μm, ensuring singly resonant oscillation. Out-coupled SRO (OC-SRO) operation is achieved by replacing mirror M_4 by a suitable output coupler (OC) across 1.6–1.7 μm. The pump beam is confocally focused to a beam radius of 63 μm ($\xi \sim 1$) at the center of the crystal. The cavity design ensures optimum overlap of pump and resonant signal at the center of the crystal ($b_p = b_s$), with a signal waist radius of 76 μm. A dichroic mirror, M, separates the generated idler from the pump.

3 Results and discussion

To study output power characteristics, the oscillator is initially configured as a SRO, and investigations of optimal out-coupling are performed by employing different OCs with signal transmissions from $T \sim 3\%$ to 6%. Figure 2 shows the simultaneously extracted idler and signal power from the OC-SRO for different OCs at a maximum available pump power of 28.6 W. The measurements were performed at the center of the tuning range for ($\Lambda = 31$ μm, 100°C). As is evident from the plot, an increase in OC transmission from 3% to 3.8% results in a rise in signal power from 7.8 W to 9.8 W, without significant compromise in idler power. Further increases in OC transmission result in the drop in signal and idler power to 7.7 W and 6 W, respectively, at 6% output coupling. As a consequence of increased output coupling, the OC-SRO threshold increases from 7.2 W at 3% to 15.4 W at 6% (inset, Fig. 2), and the intracavity signal power estimated from the OC transmission varies from 259 W ($T \sim 3\%$) to 129 W ($T \sim 6\%$). For optimal output coupling of ~3.8%, a maximum signal power of 9.8 W (at 1627 nm) together with 7.7 W of idler (at 3070 nm) is extracted for 28.6 W of input power at a pump depletion of 69.4%. Under this condition, the OC-SRO threshold is 10.5 W. So, the available pump power enables OC-SRO operation at ~2.74

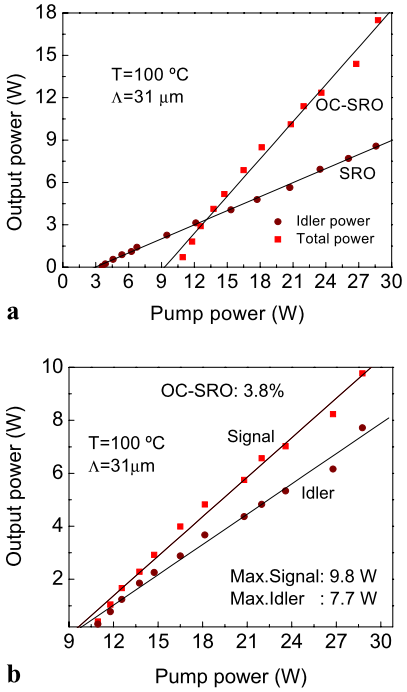

Fig. 3 (**a**) Total extracted output power as a function of pump power from SRO and OC-SRO. (**b**) Power scaling of signal and idler in OC-SRO at a temperature of 100 μC, $\Lambda = 31$ μm

times threshold where a maximum pump depletion is theoretically predicted [13, 14], confirming that this is the optimum output coupling for our device. We investigated power scaling of the optimal OC-SRO ($T \sim 3.8\%$) compared with the SRO, for the same grating period ($\Lambda = 31$ μm, 100°C), as shown in Fig. 3(a). For the SRO, an idler power up to 8.6 W was obtained at 3061 nm for 28.6 W of pump at 30% extraction efficiency, with a threshold of 3.6 W and a pump depletion of 79%. No saturation of idler power was observed at this power level. On the other hand, with the optimal OC-SRO, we were able to generate a total power of 17.5 W (9.8 W signal at 1627 nm, 7.7 W idler at 3070 nm) at an overall extraction efficiency of 61%. Figure 3(b) shows the simultaneous power scaling of signal and idler in the OC-SRO. Given a pump depletion of 69.4%, this means that 88% of the down-converted pump is successfully extracted as output. We monitored the signal wavelength using a spectrum analyzer with a resolution of 0.1 nm. In SRO operation at higher pump power level, together with the peak at the expected signal wavelength, we also observed additional spectral components red-shifted towards the longer wavelength by nearly 12 nm, but we did not observe any blue-shifted peaks. For example, when pumping at the maximum power of 28.6 W, a signal wavelength of 1631 nm and an additional peak at 1643 nm were observed at 100°C for a grating period of 31 μm. The observed additional spectral components are attributed to Raman lasing [5] or cascaded nonlinear processes [10]. On the other hand, when operating in the OC-SRO configuration, no such additional spectral components were observed, due to the significantly reduced intracavity signal intensity suppressing Raman lasing and cascaded nonlinear effects below threshold. For example, the estimated intracavity power reduces from >600 W at 100°C, corresponding to a signal wavelength of 1631 nm in the SRO, to 257 W in the OC-SRO for 3.8% OC at the same temperature, corresponding to a signal wavelength of 1627 nm. Hence, no additional spectral components were observed in the OC-SRO configuration. Given the lack of a suitable interferometer in our laboratory, we were unable to measure the linewidth of the signal and idler. However, we measured the wavelength of the idler using a wavemeter (Bristol, 721B-MIR, resolution 0.001 nm) and observed no variation in the measured wavelength over tens of seconds, implying an idler linewidth narrower than the resolution limit of the wavemeter. Given the single-frequency nature of the fiber laser pump source with typical linewidth of 100 kHz, we expect the generated signal and idler waves from the OC-SRO to also be single-mode, which is an essential requirement for spectroscopy and trace gas sensing. However, further confirmation of the single-frequency nature of the OC-SRO output requires a suitable high resolution scanning Fabry–Pérot interferometer.

We also characterized the output power of the SRO and OC-SRO across the full tuning range by varying the temperature of the MgO:PPLN crystal. In the SRO, by changing the temperature from 55°C to 200°C, we generated idler wavelengths across 3147–2787 nm, providing a total tuning of 360 nm, as shown in Fig. 4(a). For a pump power of 28.6 W, idler powers >7 W and pump depletions >65% were recorded over almost the entire tuning range, except for a drop in the idler power around 2.8 μm, corresponding to the OH^- absorption in MgO:PPLN. However, we were not able to tune the device down to room temperature, because of heavy thermal loading of the crystal.

In the OC-SRO, by employing an OC of $T \sim 3$–5% in 1.6–1.7 μm range, idler tuning over 3196–2803 nm together with signal tuning across 1594–1714 nm was obtained, enabling room-temperature operation of OC-SRO at 31°C with a total power of 15.7 W (9.1 W of signal at 1594 nm, 6.6 W of idler at 3196 nm), as shown in Fig. 4(b). Thus, the use of output coupling extended the idler wavelength range by 33 nm compared to SRO. Using the OC-SRO , we were also able to extract signal powers from 9.1 W at 1594 nm (31°C) to 7.3 W at 1714 nm (200°C), with the corresponding idler power varying from 6.6 W at 3196 nm to 5.6 W at 2803 nm. The OC values were not optimized at each wavelength, so still higher powers across the tuning range are expected. The drop in signal and idler power at higher temperatures is due to the lower OC transmission for the corresponding wavelengths and the dip around 2.8 μm is again due to the OH^- absorption in MgO:PPLN. Hence, output coupling not only

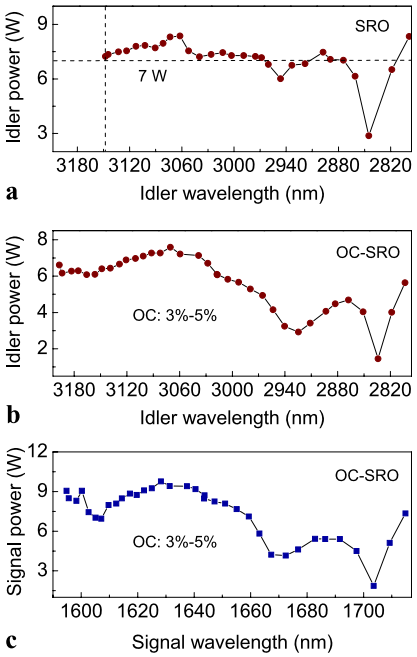

Fig. 4 Output power and temperature tuning range of (**a**) SRO idler, (**b**) OC-SRO idler, and (**c**) OC-SRO signal with ∼3–5% output coupling

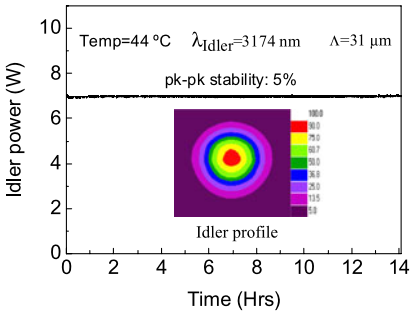

Fig. 5 Long-term power stability and far-field spatial profile of the idler beam from OC-SRO at 44°C corresponding to 3174 nm

increases the overall extraction efficiency and helps manage thermal effects, but also extends the tunability of the device. Also observed is a significant shift in idler wavelength generated in the OC-SRO compared to that at a similar temperature in SRO, which confirms the effect of crystal heating in the SRO and its efficient management by optimal output coupling in the OC-SRO. For example, near 100°C, the idler wavelength is measured as 3061 nm and 3070 nm in the SRO and OC-SRO, respectively, indicating an increase of 9 nm in the idler wavelength in the optimal OC-SRO ($T \sim 3.8\%$) compared to SRO. This corresponds to a temperature drop of ∼5°C in MgO:PPLN, as calculated from the Sellmeier equations [15].

We also investigated the power stability of the device in the two configurations at the maximum generated idler power. For the SRO, at a temperature of 100°C (idler at 3061 nm), we measured a stability of 17.4 % over 1 hour. For the OC-SRO, at a temperature 100°C (idler at 3070 nm), we recorded a peak-to-peak stability of 13.6 % over 1 hour. However, in the OC-SRO, at a temperature of 44°C (idler at 3174 nm), we measured a long-term peak-to-peak stability of 5% over 14 hours at 7 W of idler power, as shown in Fig. 5. The corresponding stability in the fiber pump laser was measured to be 0.5% over 10 hours. We attribute the improved stability of the OC-SRO at 44°C to the better temperature control of the nonlinear crystal. It was observed that the smaller the difference between the set oven temperature and the ambient temperature, the better the stability of the oven. Therefore, maintaining a constant oven temperature at a high temperature is more difficult than that close to room temperature. We believe this is the main reason for improved power stability close to room temperature. We did not observe any degradation in power stability or output beam quality over the measurement period, thus confirming the absence of photorefractive damage in the crystal even at such high power levels. We can thus conclude that the improvement in power stability is due to better control of crystal temperature close to room temperature, confirming another important advantage of the OC-SRO. It has been shown that, by careful thermal control of the nonlinear crystal, long-term power stability can be achieved without the need for an intracavity etalon or actively stabilizing the OPO with an external reference cavity [4]. Hence, similar improvement in the power stability is also to be expected by employing a temperature controller with stability better than ±0.1°C or by using a thermo-electric cooler. In the SRO configuration, the minimum operating temperature could not be reduced below 55°C due to the heavy thermal loading of the crystal in the absence of signal output coupling. We measured the quality factors of the output beam from the OC-SRO, where we obtained $M_x^2 \sim 1.28$ and $M_y^2 \sim 1.22$ for the idler at 3070 nm and $M_x^2 \sim 1.29$ and $M_y^2 \sim 1.37$ for the signal at 1627 nm. For the SRO, we obtained $M_x^2 \sim 1.3$ and $M_y^2 \sim 1.22$ for idler at 3061 nm. We attribute the larger M^2 value for the signal to the stronger impact of the thermal lens on the signal beam quality than that of the idler. The thermal lens itself is caused primarily by the absorption of the high intracavity signal field, although absorption at pump and idler wavelengths cannot be completely ruled out. Since the signal is a resonant mode of the SRO cavity, it is expected to be highly sensitive to small changes in mode-matching with the pump, as well as changes in the cavity stability conditions caused by the intracavity thermal lens formed in the crystal. On the other hand, the idler is generated in a single pass through the crystal as a result of mixing between the single-pass pump and the resonant signal beam. As such, the effect of the thermal lens is expected to be less detrimental to the quality of the idler beam than that of the signal, and so the impact on the M^2 value of idler is not

as severe as that on the M^2 value of the signal beam. Also shown in the inset of Fig. 5 is the spatial profile of the idler beam from the OC-SRO at 44°C and at 7 W, measured at a distance of 1 m away from the output, using a pyroelectric beam profiler. The measurement confirms a TEM_{00} spatial mode.

4 Conclusions

In conclusion we have demonstrated a stable, high-power, fiber-laser-pumped, cw optical parametric oscillator in the OC-SRO configuration, which can provide 17.5 W of power in the near- to mid-IR infrared at an external efficiency of 61%, with nearly 90% of down-converted pump power extracted as useful output. This compares with a total output power of 8.6 W at 30% extraction efficiency in the SRO configuration. The OC-SRO provides 513 nm of total useful tuning (idler plus signal) compared with 360 nm (idler only) in the SRO, can operate down to 44°C, delivers TEM_{00} beam quality, and exhibits long-term power stability of 5% over 14 hours. Further improvements in power and stability are possible by optimizing output coupling across the tuning range and providing better isolation from mechanical vibrations.

Acknowledgements This work was supported by the Ministry of Science and Innovation, Spain, through grant TEC2009-07991 and the Consolider project (CSD2007-00013). We also acknowledge partial support by the European Office of Aerospace Research and Development (EOARD), USA, through grant FA8655-09-1-3017 and the European Union 7th Framework Program through project MIRSURG (224042).

References

1. S.M. Cristescu, S.T. Persijn, S. Te Lintel Eckert, F.J.M. Harren, Appl. Phys. B, Lasers Opt. **92**, 343 (2008)
2. D. Chen, T.S. Rose, CLEO, CThQ2 (2005)
3. S.T. Lin, Y.Y. Lin, Y.C. Huang, A.C. Chiang, J.T. Shy, CLEO, CTull (2008)
4. M. Vainio, J. Peltola, S. Persijn, F.J.M. Harren, L. Halonen, Appl. Phys. B, Lasers Opt. **94**, 411 (2009)
5. A. Henderson, R. Stafford, Opt. Lett. **32**, 1281 (2007)
6. M.M.J. van Herpen, S. Li, S.E. Bisson, S. Te Lintel Hekkert, F.J.M. Harren, Appl. Phys. B, Lasers Opt. **75**, 329 (2002)
7. P. Gross, M.E. Klein, T. Walde, K.-J. Boller, M. Auerbach, P. Wessels, C. Fallnich, Opt. Lett. **27**, 418 (2002)
8. I.D. Lindsay, B. Adhimoolam, P. Groß, M. Klein, K. Boller, Opt. Express **13**, 1234 (2005)
9. M. Vainio, M. Siltanen, J. Peltola, L. Halonen, Opt. Express **17**, 7702 (2009)
10. J. Kiessling, R. Sowade, I. Breunig, K. Buse, V. Dierolf, Opt. Express **17**, 87 (2009)
11. G.K. Samanta, M. Ebrahim-Zadeh, Opt. Express **16**, 6883 (2008)
12. G.K. Samanta, M. Ebrahim-Zadeh, Opt. Lett. **33**, 1228 (2008)
13. L.B. Kreuzer, in *Proc. Joint Conf. Lasers and Opt.-Elect.*, p. 52 (1969)
14. R. Sowade, I. Breunig, J. Kiessling, K. Buse, Appl. Phys. B, Lasers Opt. **96**, 25 (2009)
15. O. Paul, A. Quosig, T. Bauer, M. Nittmann, J. Bartschke, G. Anstett, J.A. L'Huillier, Appl. Phys. B, Lasers Opt. **86**, 111 (2007)